

DOI:10.1002/ejic.201201022

Synthesis and Reactivity Studies of Dicationic Dihydrogen Complexes Bearing Sulfur-Donor Ligands: A Combined Experimental and Computational Study

Thirumanavelan Gandhi,*^[a] Subramani Rajkumar,^[a]
V. Prathyusha,^[b] and U. Deva Priyakumar*^[b]

Keywords: Ruthenium / Dihydrogen ligands / S ligands / Phosphane ligands / Density functional calculations

A series of dihydrogen complexes *trans*-[Ru(η^2 -H₂){SC(SR)H}(dppe)₂][X][BF₄] (R = CH₃, X = OTf; R = C₆H₅CH₂, X = BPh₄; R = H₂C=CHCH₂, X = BPh₄; dppe = Ph₂PCH₂CH₂PPh₂) bearing sulfur-donor ligands has been synthesized by protonation of the (alkyl dithioformate)hydrido complexes *trans*-[Ru(H){SC(SR)H}(dppe)₂][X] by using HBF₄·Et₂O. Competitive substitution reactions between H₂ and SC(SR)H in *trans*-[Ru(η^2 -H₂){SC(SR)H}(dppe)₂][X][BF₄] have been studied by treatment with CH₃CN, CO, and P(OCH₃)₃. These resulted in the expulsion of SC(SR)H from the metal center, thus indicating that the alkyl dithioformate ligand is more labile than

H₂. Bonding of alkyl dithioformate ligands (sulfur-donor ligands) *trans* to H₂ have been studied by comparing the H–H distances and chemical-shift values (¹H NMR spectroscopy) of the various dihydrogen complexes bearing different *trans* ligands. This study qualitatively suggests that the alkyl dithioformate ligands in these *trans*-dihydrogen complexes show a poor π effect, and it is further supported by density functional theory calculations. The first example of a dihydrogen complex bearing dithioformic acid, *trans*-[Ru(η^2 -H₂){SC(SH)H}(dppe)₂][BF₄]₂, was obtained by protonation of *trans*-[Ru(H){SC(S)H}(dppe)₂] by using HBF₄·Et₂O.

Introduction

The chemistry of dihydrogen complexes that bear co-ligands, especially ligands *trans* to H₂, such as CO,^[1] halides,^[2] phosphanes, phosphites,^[3] cyanides,^[4] and nitriles,^[5] has been well established. On the contrary, dihydrogen complexes bearing sulfur-donor ligands have not been well explored. Esteruelas and co-workers^[6] reported the first examples of dihydrogen complexes containing sulfur-donor ligands. They treated [Os(H)₂Cl₂(PiPr₃)₂] with K[EtOCS₂] to obtain the dihydrogen complexes [Os(η^2 -H₂){ η^2 -S₂C(OMe)}(Cl)(PiPr₃)₂] and [Os(η^2 -H₂)(PiPr₃)₂(EtOCS₂){ η^2 -S₂C(OEt)}], and their H–H distances were determined from the spin–lattice relaxation time measurements. Albéniz et al.^[7] have shown that the dihydrogen complex [Os(η^2 -H₂)(CO)(η^2 -S₂CH)(PiPr₃)₂][BF₄] could be prepared by protonation of [Os(H)(CO)(η^2 -S₂CH)(PiPr₃)₂] with HBF₄·Et₂O in CD₂Cl₂. The H–H distance in [Os(η^2 -H₂)(CO)(η^2 -S₂CH)(PiPr₃)₂][BF₄] was calculated from the $T_{1(\min)}$ and

the $J_{H,D}$ values of its η^2 -HD isotopomer. The groups of Sellmann^[8,9] and Morris^[10] prepared dihydrogen transition-metal complexes that bear sulfur-donor ligands, which are biologically relevant to enzyme hydrogenases and nitrogenases. Sellmann et al.^[8] reported dihydrogen complexes with sulfur-rich coordination spheres. [Ru(η^2 -H₂)(“S₄”)(PCy₃)] {“S₄”²⁻ = 1,2-bis[(2-mercaptophenyl)thioethane]²⁻} and its η^2 -HD isotopomer were obtained by treatment of [Ru(H)(“S₄”)(PCy₃)]⁻ with CH₃OH and CD₃OD, respectively, and its $J_{H,D}$ value was found to be 32 Hz. In another report, Sellmann and co-workers^[9] reported the preparation of the dihydrogen complex [Ru(η^2 -H₂)(“N₂Me₂S₂”)(PR₃)] [“N₂Me₂S₂” = 1,2-ethanediamine-*N,N'*-dimethyl-*N,N'*-bis(2-benzenethiolate)²⁻; R = *i*Pr, Cy] by substitution of N₂ in [Ru(N₂)(“N₂Me₂S₂”)(PR₃)] with H₂. Schlaf et al.^[10] reported the synthesis of dihydrogen complexes bearing sulfur-donor ligands of the type [M(η^2 -H₂)(CO)(L)(PPh₃)₂][BF₄] (M = Ru, Os; L = pyridine-2-thiolate, quinoline-8-thiolate) by protonating their precursor hydrido complexes with HBF₄·Et₂O. They prepared *trans*-[Os(η^2 -H₂)(HSPH)(dppe)₂][BF₄]₂ (dppe = Ph₂PCH₂CH₂PPh₂) by protonation of the *trans*-[Os(H)(HSPH)(dppe)₂][BF₄] complex by using HBF₄·Et₂O.^[10] Here we present the synthesis and properties of new (dihydrogen)ruthenium complexes bearing sulfur-donor ligands of the type *trans*-[Ru(η^2 -H₂){SC(SR)H}(dppe)₂][X][BF₄] (R = CH₃, X = OTf; R = C₆H₅CH₂, X = BPh₄; R = CH₂=CHCH₂, X = BPh₄; R = H, X = BF₄).

Computational tools have been shown to be indispensable in studying the structural and energetic properties of

[a] Materials Chemistry Division,
School of Advanced Sciences, VIT University,
Vellore 632014, India
E-mail: velan.g@vit.ac.in
Homepage: <http://vit.ac.in/sas/faculty.asp>

[b] Centre for Computational Natural Sciences and Bioinformatics,
International Institute of Information Technology,
Hyderabad 500032, India
E-mail: deva@iiit.ac.in
<http://www.iiit.ac.in/people/faculty/deva>

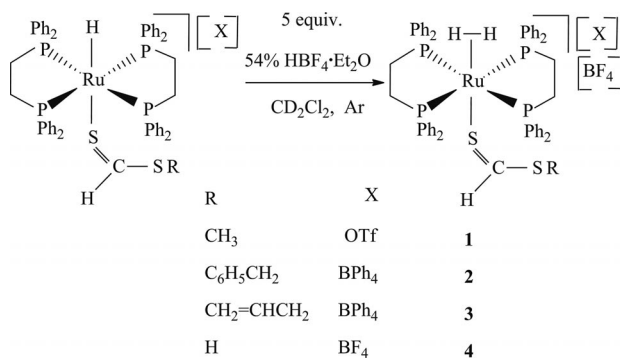
Supporting information for this article is available on the WWW under <http://dx.doi.org/10.1002/ejic.201201022>.

transition-metal complexes in general.^[11] Density functional studies were used to investigate and predict the geometries, metal–ligand bonding,^[12] and $J_{H,D}$ values in molecular dihydrogen complexes.^[13] Furthermore, it supports the H_2 activation mechanism,^[14] exchange processes between $M(H)(H_2)$,^[15] and the acidity of the dihydrogen complexes.^[16] In this paper, we have used hybrid density functional calculations at the B3LYP level of theory to study the Ru^{2+} complexes. The $Ph_2P(CH_2)_2PPh_2$ ligand has been replaced by the $H_2P(CH_2)_2PH_2$ ligand for computational studies. The substitution of the phenyl group in the ligand by a hydrogen atom is commonplace in computational studies and has been shown to have only a moderate effect on the structural properties of the system under consideration.^[17–19] Similarly, PH_3 and PMe_3 have been shown to satisfactorily model the PPh_3 ligand.^[20,21] Additionally, we have performed natural bond orbital (NBO) and atoms-in-molecules (AIM) analyses to specifically study the nature of bonding between the Ru^{2+} ion and ligands, especially how the behavior of the dihydrogen ligand changes with respect to the ligand present *trans* to H_2 .

Results and Discussion

Synthesis and Characterization of *trans*- $[Ru(\eta^2-H_2)\{SC(SR)H\}(dppe)_2][X][BF_4]$ ($R = CH_3$, $X = OTf$; $R = C_6H_5CH_2$, $X = BPh_4$; $R = CH_2=CHCH_2$, $X = BPh_4$; $R = H$, $X = BF_4$)

The protonation of hydrido complexes *trans*- $[Ru(H)\{SC(SR)H\}(dppe)_2][X]$ ($R = CH_3$, $X = OTf$; $R = C_6H_5CH_2$, $X = BPh_4$; $R = CH_2=CHCH_2$, $X = BPh_4$; $R = H$, $X = BF_4$) with 54% $HBF_4 \cdot Et_2O$ (5 equiv.) afforded the corresponding dihydrogen complexes *trans*- $[Ru(\eta^2-H_2)\{SC(SR)H\}(dppe)_2][X][BF_4]$ [$R = CH_3$, $X = OTf$ (**1**); $R = C_6H_5CH_2$, $X = BPh_4$ (**2**); $R = CH_2=CHCH_2$, $X = BPh_4$ (**3**); $R = H$, $X = BF_4$ (**4**)] [Equation (1)]. Addition of less than 5 equiv. of 54% $HBF_4 \cdot Et_2O$ to complexes **1**, **2**, **3**, and **4** led to incomplete protonation of the hydrides, and equilibrium is thereby established between the hydrido and its corresponding dihydrogen complexes. A broad peak at $\delta = 11.50$ ppm in the 1H NMR spectra corroborates the presence of an excess amount of $HBF_4 \cdot Et_2O$ (Figure 1). These reactions were carried out in CD_2Cl_2 under argon. The dihydrogen complexes were characterized in solution by using



NMR spectroscopy since attempts to isolate these derivatives in the solid state resulted in their decomposition. The bound H_2 appears as a broad singlet in the range $\delta = -8.55$ to -8.71 ppm in the 1H NMR spectrum. These signals are shifted downfield with respect to the starting hydrido complexes. The $^{31}P\{^1H\}$ NMR spectra of the dihydrogen complexes comprise only a singlet resonance, thus indicating equivalent phosphorus nuclei with a *trans* geometry for the dihydrogen and the alkyl dithioformate/dithioformic acid ligands.

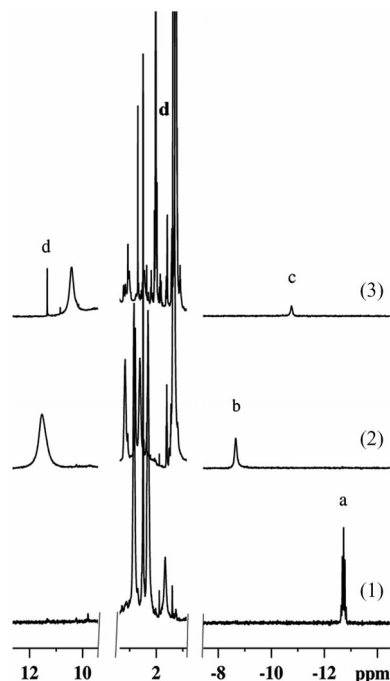


Figure 1. Stack plot of the 1H NMR spectra of the reaction of *trans*- $[Ru(\eta^2-H_2)\{SC(SCH_3)H\}(dppe)_2][OTf][BF_4]$ (**1**) with CH_3CN in $CDCl_3$. (1) *trans*- $[Ru(H)\{SC(SCH_3)H\}(dppe)_2][OTf]$; (2) *trans*- $[Ru(H)\{SC(SCH_3)H\}(dppe)_2][OTf]$ + 54% $HBF_4 \cdot Et_2O$; (3) *trans*- $[Ru(\eta^2-H_2)\{SC(SCH_3)H\}(dppe)_2][OTf][BF_4]$ + CH_3CN . (a) *trans*- $[Ru(H)\{SC(SCH_3)H\}(dppe)_2][OTf]$; (b) *trans*- $[Ru(\eta^2-H_2)\{SC(SCH_3)H\}(dppe)_2][OTf][BF_4]$; (c) *trans*- $[Ru(\eta^2-H_2)(CH_3CN)(dppe)_2][OTf][BF_4]$; and (d) $SC(SCH_3)H$.

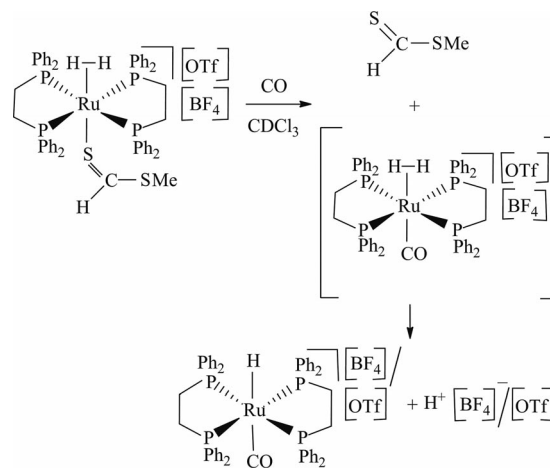
The dihydrogen complexes bearing sulfur-donor ligands such as thiolates,^[8–10] thiols,^[22] η^2 -dithioformates,^[7] xanthate derivatives, and thiocarboxylate derivatives^[6] have been reported; however, dihydrogen complexes bearing alkyl dithioformates and dithioformic acid are unknown. Complex **4** is the first example of a dicationic dihydrogen complex bearing the unstable dithioformic acid as the *trans* ligand.^[23] Dithioformic acid is an unstable species; it has been studied extensively by theoretical methods,^[24] microwave spectroscopy,^[25] and IR spectroscopy.^[26]

Reactivity of *trans*- $[Ru(\eta^2-H_2)\{SC(SCH_3)H\}(dppe)_2][OTf][BF_4]$ with CH_3CN

Treatment of a solution of **1** in $CDCl_3$ with CH_3CN (2 equiv.) afforded the dicationic dihydrogen complex *trans*- $[Ru(\eta^2-H_2)(CH_3CN)(dppe)_2][OTf][BF_4]$ by means of the eli-

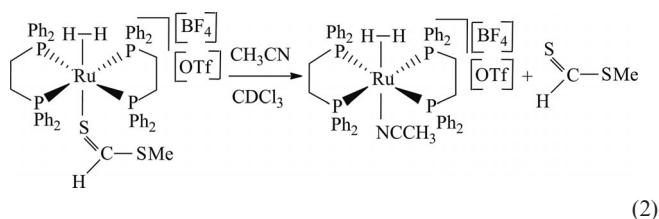
mination of the *trans*-SC(SCH₃)H ligand [Equation (2)]. This is surprising since the bound H₂ ligand would be expected to be more labile than the methyl dithioformate moiety. The progress of this substitution reaction was monitored by both ¹H and ³¹P NMR spectroscopy. Addition of 1 equiv. of CH₃CN to **1** resulted in the formation of *trans*-[Ru(η²-H₂)(CH₃CN)(dppe)₂][OTf][BF₄] and free SC(SCH₃)H, as shown in the Figure 1. It was found from the ¹H NMR spectra that treatment of **1** with CH₃CN yielded only 80% of *trans*-[Ru(η²-H₂)(CH₃CN)(dppe)₂][OTf][BF₄]. The ¹H NMR spectrum of *trans*-[Ru(η²-H₂)(CH₃CN)(dppe)₂][OTf][BF₄] shows a broad singlet at δ = -10.77 ppm, which is comparable to that of the reported *trans*-[Ru(η²-H₂)(CH₃CN)(dppe)₂][BF₄]₂.^[5] The other possible product is CH₃CN *trans* to methyl dithioformate {i.e., *trans*-[Ru(CH₃CN){SC(SCH₃)H}(dppe)₂][OTf][BF₄]} with the expulsion of H₂; this species was not observed because of steric crowding generated by *trans* ligands CH₃CN and methyl dithioformate. There have been only very few examples in the literature in which the dihydrogen ligand stays intact with the metal center, and other coligands undergo a substitution reaction. Esteruelas and co-workers^[27] reported that the η²-H₂ ligand of [Os¹{C₆H₄(O¹)CH₃}(η²-H₂)(H₂O)(PiPr₃)(Os¹-O¹)] [BF₄] stays intact upon addition of acetone oxime. However, the aqua ligand is replaced by acetone oxime to yield [Os¹{C₆H₄(O¹)CH₃}(η²-H₂){N(OH)=C(CH₃)₂}(PiPr₃)(Os¹-O¹)] [BF₄] derivative. The methyl dithioformate binds to the metal atom through the lone pair of electrons present on the sulfur atom as in thioethers^[28] and thioureas.^[29] The bonding of the alkyl dithioformate to the metal atom will be discussed in detail in the latter part of this article. It is instructive to note from this result that the alkyl dithioformate ligand is more labile than the bound H₂.

occurs to yield the hydrido derivative, and a proton equivalent is released, which migrates to an external Lewis base or an ancillary ligand or anion.^[31] Mezzetti and co-workers observed *trans*-[Ru(η²-H₂)(CO)(dppe)₂][OTf][BPh₄] at only 233 K by protonation of *trans*-[Ru(H)(CO)(dppe)₂][BPh₄] with HOTf.^[1e] The bound H₂ ligand in this derivative was shown to be highly activated toward heterolysis.



Scheme 1.

This reactivity pattern (Scheme 1) was studied by using NMR spectroscopy. Figure 2 [see plot (2)] shows the formation of **1** by protonation of *trans*-[Ru(H){SC(SCH₃)H}(dppe)₂][OTf] with HBF₄·Et₂O. Purging CO through the solution of **1** resulted in the decrease in concentration of **1**, with a concomitant increase in the concentration of *trans*-[Ru(H)(CO)(dppe)₂][OTf]/[BF₄] as shown in Figure 2 [see plot (3)] and the reaction is complete in 15 min [see plot (4)]. The hydrido ligand of *trans*-[Ru(H)(CO)(dppe)₂]-



Reactivity of *trans*-[Ru(η²-H₂){SC(SCH₃)H}(dppe)₂][OTf][BF₄] (**1**) with CO

Purging CO gas at a steady rate through a solution of **1** in CDCl₃ for 2 min led to the formation of *trans*-[Ru(H)(CO)(dppe)₂][OTf]/[BF₄] accompanied by the elimination of methyl dithioformate and a proton equivalent (Scheme 1). The product *trans*-[Ru(H)(CO)(dppe)₂][OTf]/[BF₄]^[30] presumably formed through the intermediacy of *trans*-[Ru(η²-H₂)(CO)(dppe)₂][OTf][BF₄], the bound H₂ ligand of which is expected to be highly acidic. Heterolytic cleavage of H₂ in *trans*-[Ru(η²-H₂)(CO)(dppe)₂][OTf][BF₄]

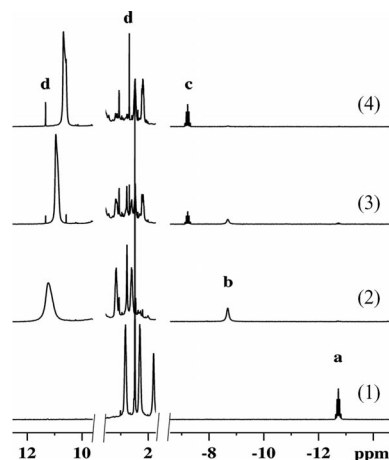


Figure 2. Stack plot of the ¹H NMR spectra of the reaction of *trans*-[Ru(η²-H₂){SC(SCH₃)H}(dppe)₂][OTf][BF₄] (**1**) with CO in CDCl₃. (1) *trans*-[Ru(H){SC(SCH₃)H}(dppe)₂][OTf]; (2) *trans*-[Ru(H){SC(SCH₃)H}(dppe)₂][OTf] + 54% HBF₄·Et₂O; (3) *trans*-[Ru(η²-H₂){SC(SCH₃)H}(dppe)₂][OTf][BF₄] + CO; (4) plot (3) + 15 min. (a) *trans*-[Ru(H){SC(SCH₃)H}(dppe)₂][OTf]; (b) *trans*-[Ru(η²-H₂){SC(SCH₃)H}(dppe)₂][OTf][BF₄]; (c) *trans*-[Ru(H)(CO)(dppe)₂][OTf]/[BF₄]; and (d) SC(SCH₃)H.

[OTf] shows a quintet at $\delta = -7.22$ ppm ($J_{H,P} = 19.6$ Hz) due to coupling with 4 equivalent phosphorus nuclei. The outcome of this reaction is also surprising since SC(SCH₃)H is replaced by CO instead of η^2 -H₂. This reaction also demonstrates that the methyl dithioformate is more labile than the bound H₂ ligand.

Reactivity of *trans*-[Ru(η^2 -H₂){SC(SCH₃)H}(dppe)₂][OTf][BF₄] with P(OCH₃)₃

When P(OCH₃)₃ (3 equiv.) was added to a solution of **1** in CDCl₃, instant deprotonation of the dihydrogen ligand was observed to yield the *trans*-[Ru(H){SC(SCH₃)H}(dppe)₂][OTf]/[BF₄] hydrido complex [Figure 3; plot (3) matches plot (1)] and protonated [HP(OCH₃)₃]⁺ in a small quantity that was unobservable [Scheme 2 (a)]. Subsequently, the excess amounts of P(OCH₃)₃ and HBF₄·Et₂O participate in the substitution of SC(SCH₃)H from *trans*-[Ru(H){SC(SCH₃)H}(dppe)₂][OTf]/[BF₄] to yield *trans*-[Ru(H){P(OCH₃)₃}(dppe)₂][OTf]/[BF₄] and conversion of P(OCH₃)₃ to PF(OCH₃)₂, respectively, both in coordinated and noncoordinated form (Scheme 2).

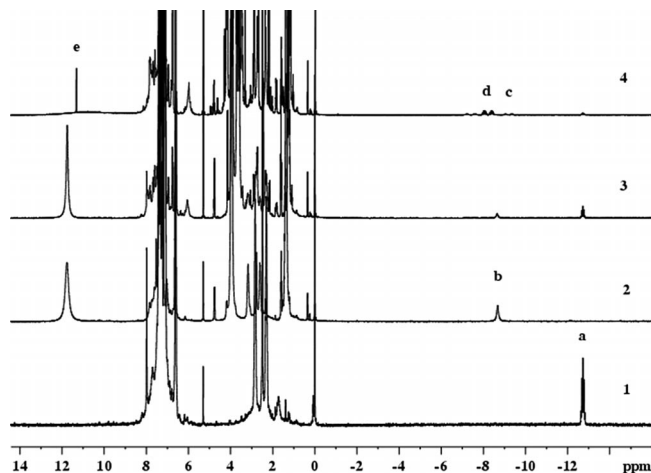
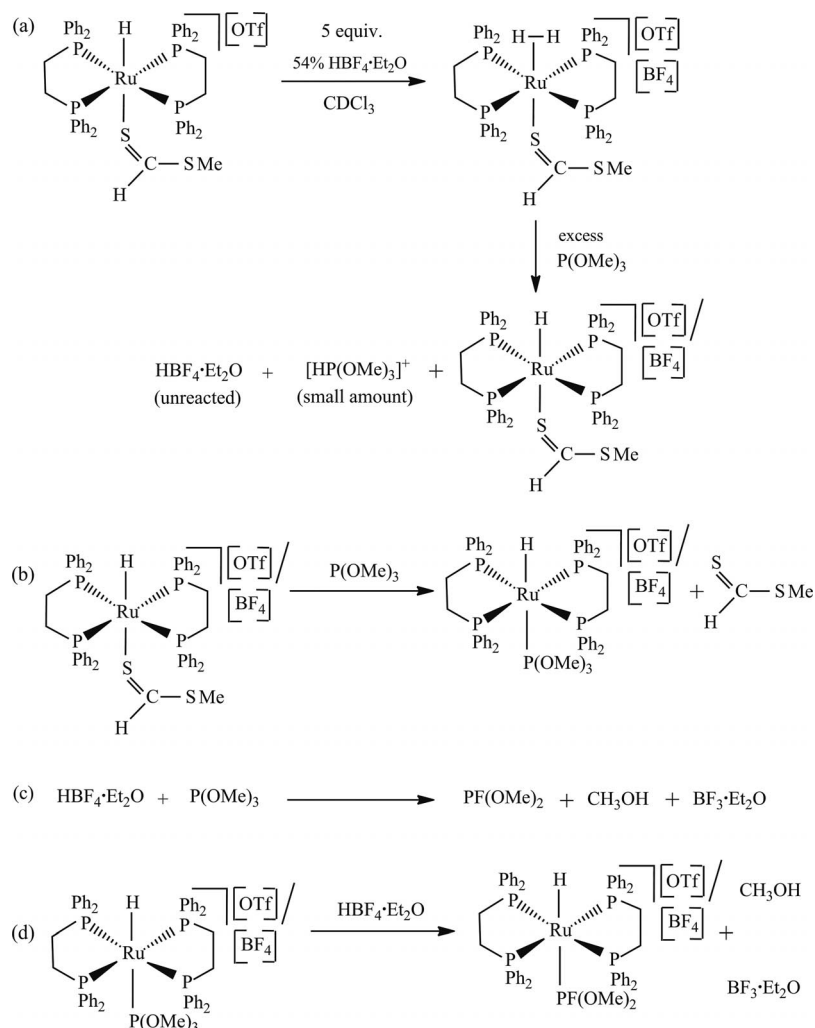


Figure 3. Stack plot of the ¹H NMR spectra of the reaction of **1** with P(OCH₃)₃ in CDCl₃. (1) *trans*-[Ru(H){SC(SCH₃)H}(dppe)₂][OTf]; (2) *trans*-[Ru(H){SC(SCH₃)H}(dppe)₂][OTf] + 54% HBF₄·Et₂O; (3) *trans*-[Ru(η^2 -H₂){SC(SCH₃)H}(dppe)₂][OTf][BF₄] + P(OCH₃)₃; (4) plot (3) + 30 min. (a) *trans*-[Ru(H){SC(SCH₃)H}(dppe)₂][OTf]; (b) *trans*-[Ru(η^2 -H₂){SC(SCH₃)H}(dppe)₂][OTf][BF₄]; (c) *trans*-[Ru(H){P(OCH₃)₃}(dppe)₂][OTf]/[BF₄]; (d) *trans*-[Ru(H){PF(OCH₃)₂}(dppe)₂][OTf]/[BF₄]; and (e) SC(SCH₃)H.



Scheme 2.

The excess amount of $P(OCH_3)_3$ present in the solution undergoes the following reactions:

(a) It displaces $SC(SCH_3)H$ from $trans-[Ru(H)\{SC(SCH_3)H\}(dppe)_2][OTf]/[BF_4]$ to yield $trans-[Ru(H)\{P(OCH_3)_3\}(dppe)_2][OTf]/[BF_4]$ and free $SC(SCH_3)H$ [Scheme 2 (b)], which was monitored both by 1H and $^{31}P\{^1H\}$ NMR spectroscopy; $trans-[Ru(H)\{SC(SCH_3)H\}(dppe)_2][OTf]/[BF_4]$ exhibits a quintet at $\delta = -12.72$ ppm for the hydrido ligand [as shown in Figure 3; plot (3) matches plot (1)], and $trans-[Ru(H)\{P(OCH_3)_3\}(dppe)_2][OTf]/[BF_4]$ appears as a doublet of quintets centered at $\delta = -9.19$ ppm for the hydrido ligand as shown in Figure 3 [see plot (4)].

(b) It reacts with $HBF_4 \cdot Et_2O$ (an excess amount of $HBF_4 \cdot Et_2O$ was used to stabilize **1**) to yield free $PF(OCH_3)_2$. The $^{31}P\{^1H\}$ NMR spectrum exhibits a doublet centered at $\delta = 132.0$ ppm for free $PF(OCH_3)_2$.^[32]

(c) Furthermore, $trans-[Ru(H)\{P(OCH_3)_3\}(dppe)_2][OTf]/[BF_4]$ with an excess amount of $HBF_4 \cdot Et_2O$ yields $trans-[Ru(H)\{PF(OCH_3)_2\}(dppe)_2][OTf]/[BF_4]$ [Scheme 2 (d)]. The driving force for the formation of $trans-[Ru(H)\{PF(OCH_3)_2\}(dppe)_2][OTf]/[BF_4]$ from $trans-[Ru(H)\{P(OCH_3)_3\}(dppe)_2][OTf]/[BF_4]$ is the cone-angle reduction of the *trans*-phosphite ligand as reported by Mathew et al.^[34] In this reaction, the OCH_3 group is likely to be protonated followed by the elimination of CH_3OH . Consequently, the BF_4^- counterion provides the F^- for the phosphite to result in the $PF(OCH_3)_2$ ligand. $trans-[Ru(H)\{P(OCH_3)_3\}(dppe)_2][OTf]/[BF_4]$ and $trans-[Ru(H)\{PF(OCH_3)_2\}(dppe)_2][OTf]/[BF_4]$ appear as a doublet of quintets and doublet of sextets centered at $\delta = -9.19$ and -8.22 ppm, respectively, for the hydrido ligands as shown in Figure 3 [see plot (4)]. The $^{31}P\{^1H\}$ NMR spectrum exhibits a doublet of quintets centered at $\delta = 134.6$ ppm for $trans-[Ru(H)\{PF(OCH_3)_2\}(dppe)_2][OTf]/[BF_4]$. All the above reactions are complete in 30 min. Thus, the methyl dithioformate moiety in $trans-[Ru(H)\{SC(SCH_3)H\}(dppe)_2][OTf]/[BF_4]$ was easily replaced by $P(OMe)_3$ [Scheme 2 (b)], and we were led to conclude that methyl dithioformate is a labile ligand.

1H NMR Spectroscopy T_1 Measurements

The variable-temperature spin–lattice relaxation times (T_1) for η^2-H_2 of $trans-[Ru(\eta^2-H_2)\{SC(SR)H\}(dppe)_2][X]$ [$R = CH_3$, $X = OTf$ (**1**); $R = C_6H_5CH_2$, $X = BPh_4$ (**2**); $R = CH_2=CHCH_2$, $X = BPh_4$ (**3**); and $R = H$, $X = BF_4$ (**4**)] were determined in CD_2Cl_2 . T_1 data were obtained in the temperature range 213–301 K and are summarized in Table 1. T_1 values reach minima at 15.1 ms at 253 and 263 K for complexes **1** and **3**, respectively. For complexes **2** and **4**, $T_{1(min.)}$ values were not observed. The H–H distances can be calculated from the T_1 minima values.^[33] Thus, the H–H distances are 1.06 and 0.84 Å, respectively, for the slow and the fast rotation regimes of the H_2 ligand for **1** and **3**.

Table 1. Variable-temperature spin–lattice relaxation times (T_1) (400 MHz) of the η^2-H_2 ligand in $trans-[Ru(\eta^2-H_2)\{SC(SR)H\}(dppe)_2][X][BF_4]$ complexes in CD_2Cl_2 . Italicized data indicate $T_{1(min.)}$.

<i>T</i> [K]	<i>T</i> ₁ [ms] 1	<i>T</i> ₁ [ms] 2 ^[a]	<i>T</i> ₁ [ms] 3	<i>T</i> ₁ [ms] 4 ^[a]
301			16.5	
293	15.8	7.2	<i>15.1</i>	15.8
283	15.8	7.2	<i>15.1</i>	15.8
273	15.8	8.6	<i>15.1</i>	15.8
263	15.8	11.5	<i>15.1</i>	15.8
253	<i>15.1</i>	14.4	<i>15.1</i>	15.8
243	15.8	17.3	<i>15.1</i>	15.8
233	15.8	20.2	15.8	17.3
223	17.3	21.6	17.3	18.7
213	18.7	30.3	18.7	20.2

[a] No $T_{1(min.)}$ was observed.

H–D Isotopomers

Deuterium was incorporated into the η^2-H_2 ligand by bubbling HD gas (generated from the reaction of NaH and D_2O) through solutions of **1**, **2**, **3**, and **4** in CD_2Cl_2 for 5 min. The η^2-HD isotopomers $trans-[Ru(\eta^2-HD)\{SC(SR)H\}(dppe)_2][X][BF_4]$ [$R = CH_3$, $X = OTf$ (**[D]1**); $R = C_6H_5CH_2$, $X = BPh_4$ (**[D]2**); $R = CH_2=CHCH_2$, $X = BPh_4$ (**[D]3**); and $R = H$, $X = BF_4$ (**[D]4**)] were thus obtained. Albeniz et al.^[34] proposed that isotopic scrambling occurs due to a combination of the lability and the acidity of the H_2 ligand. The η^2-HD signals were observed in the 1H NMR spectra by nullifying the resonance due to the η^2-H_2 ligand by the inversion recovery method using the relationship $T_1 = \tau_{null}/\ln 2$ and the known T_1 values of the dihydrogen complexes at room temperature.^[22,35,36] The $J_{H,D}$ values together with the H–H distances for these complexes are summarized in Table 2. $J_{H,D}$ values for all the η^2-HD derivatives are 28.4 Hz, and the corresponding d_{H-H} is 0.94 Å, which was calculated by using the equation $d_{H-H} = -0.0167 J_{H,D} + 1.42$ developed by Morris.^[35b] Similar d_{H-H} values for complexes **[D]1** to **[D]4** corroborate that there is no significant change in electronics at the metal center by changing the R group in the alkyl dithioformate moiety. Sellmann and co-workers observed $J_{H,D}$ values of 32 Hz for dihydrogen complexes bearing sulfur-donor ligands of the type $[Ru(\eta^2-H_2)(PCy_3)(“S_4”)]$ {“ S_4 ”²⁻ = 1,2-bis[(2-mercaptophenyl)thioethane]²⁻}, which is larger than the coupling constants obtained in our complexes.^[8]

Table 2. H–H distances of the η^2-H_2 ligand of complexes $trans-[Ru(\eta^2-H_2)\{SC(SR)H\}(dppe)_2][X][BF_4]$ obtained from $J_{H,D}$.

R (compound)	$J_{H,D}$ [Hz]	d_{H-H} [Å]
CH_3 ([D]1)	28.4	0.94
$C_6H_5CH_2$ ([D]2)	28.4	0.94
$CH_2=CHCH_2$ ([D]3)	28.4	0.94
H ([D]4)	28.4	0.94

The η^2-HD resonances of complexes **[D]1**, **[D]2**, **[D]3**, and **[D]4** experience downfield shifts relative to their η^2-H_2 counterparts in the 1H NMR spectra, and these shifts are of the order of 134–186 ppb. The η^2-HD isotopomers of

many dihydrogen complexes reported in the literature exhibit upfield shifts relative to their $\eta^2\text{-H}_2$ analogues. On the contrary, the ones that show downfield shifts are very few.^[37] These small chemical-shift differences are essentially independent of temperature, thereby suggesting that there is only one structure for these dicationic complexes.^[38] A rapid equilibrium between a dihydrido and a dihydrogen structure would likely lead to temperature-dependent isotope effects that result from isotopic perturbation of equilibrium.^[39]

Bonding of S Ligands to the Metal Atom in the *trans*-[Ru($\eta^2\text{-H}_2$){SC(SR)H}(dppe)₂][X][BF₄] Complexes [R = CH₃, X = OTf (1); R = C₆H₅CH₂, X = BPh₄ (2); R = CH₂=CHCH₂, X = BPh₄ (3); R = H, X = BF₄ (4)]: Experimental and Computational Studies

Bonding of H₂ to a metal atom is described by the $\sigma(\eta^2\text{-H}_2)$ donation of electron to the empty d(M) orbital and π back-donation from the filled d(M) orbital to the $\sigma^*(\eta^2\text{-H}_2)$ orbital. The properties and reactivity of the metal-bound H₂ molecule greatly depend on the ligand bound *trans* to it. If the *trans* ligand is a π -donor (Cl⁻), it favors the $\sigma(\eta^2\text{-H}_2)$ donation to the d(M) orbital and increases the π back-donation from the d(M) orbital to the $\sigma^*(\eta^2\text{-H}_2)$ orbital, which results in a long H–H bond. If the *trans* ligand is a π -acceptor [CO, PF(OR)₂, PF₃], it reduces the π back-donation from the d(M) orbital to the $\sigma^*(\eta^2\text{-H}_2)$ orbital, which results in either a short H–H bond or heterolytic cleavage. If the *trans* ligand is a strong σ -donor (H⁻), there is a powerful *trans* labilizing effect that reduces $\sigma(\eta^2\text{-H}_2)$ donation, which once again weakens the M–($\eta^2\text{-H}_2$) binding and contracts $d_{\text{H-H}}$.^[40]

Table 3 shows a comparison of chemical shifts and H–H bond lengths of our complexes and others. One thing common to all these complexes (listed in Table 3) is that dihydrogen is bound to the ruthenium atom and has the same diphosphane (dppe) ligand except for a CO complex (dppp), but the variable is the *trans* ligand. The chemical-shift values and the H–H bond lengths of dihydrogen complexes bearing *trans*-sulfur ligands (alkyl dithioformate/dithioformic acid) lie in between those that have the π -donor (Cl⁻), and π -acceptor [CO, PF₃, PF(OR)₂] and σ -donor ligands (H⁻) (Table 3). This qualitatively suggests that the sulfur ligands *trans* to $\eta^2\text{-H}_2$ in complexes **1**, **2**, **3**, and **4** are both good π -donor and π -acceptor ligands, thus showing a synergistic effect. The following section provides the results

from the density functional theory calculations and the discussion of the bonding in these complexes determined on the basis of the results.

The H–H bond lengths of the dihydrogen ligand in each of the complexes were calculated, and compared with the estimates obtained by using the NMR spectroscopic chemical-shift values (Table 4). The distance between the two hydrogen atoms obtained using experimental data is the maximum for the π -donor ligand (Cl⁻), and the minimum for the π -acceptor ligand (CO). For the other ligands, the distances were found to be intermediate between the two values. Such a trend of the change in the bond lengths with respect to the nature of the ligand is accurately captured by the computational methods used here. The $\eta^2\text{-H}_2$ bond length seems to depend on the *trans* ligand bound to the metal center. For a π -donor (Cl⁻) ligand, the π back-donation from the d(M) orbital to the $\sigma^*(\eta^2\text{-H}_2)$ increases resulting in a longer H–H distance. On the other hand, when the ligand bound *trans* to H₂ is a π -acceptor (e.g., CO), then the π back-donation from the d(M) orbital to $\sigma^*(\eta^2\text{-H}_2)$ decreases, thereby resulting in a shorter H–H bond. Such an electronic effect is further confirmed on the basis of NBO and AIM analyses (see below). Comparison of the experimental and the computed bond lengths reveals that the B3LYP/LANL2DZ method seems to underestimate the bond lengths in general, which might be because of one or more of the following two reasons: (a) the computations were performed in the gas phase, and the experiments were performed in the presence of a solvent; (b) the bidentate ligand Ph₂PCH₂CH₂PPh₂, which was used in the experimental study, has been replaced by H₂PCH₂CH₂PH₂. Irrespective of such quantitative differences, the qualitative trends, and hence the conclusions from the computational study are not expected to change with respect to the change in the conditions or the level of theory used. The pK_a value that corresponds to the SH group of the ligand is expected

Table 4. Experimental estimates of the H–H bond length [Å] and interaction energies corresponding to the π back-donation from Ru to the dihydrogen moiety calculated by using the second-order perturbation analysis with the NBO method.

<i>trans</i> Ligand	$d_{\text{H-H}}$ [Å]		π Back-donation (Ru→H ₂) [kcal mol ⁻¹]
	Exp.	B3LYP	
Cl ⁻	0.98	0.843	21.10
SC(SCH ₃)H	0.94	0.825	15.77
H ⁻	0.88	0.797	11.25
CO	0.85	0.793	7.98

Table 3. Chemical-shift values and H–H bond lengths of *trans*-[Ru($\eta^2\text{-H}_2$)(L)(diphos)₂]²⁺.

<i>trans</i> -Ligand (L)	Ancillary ligand (diphos)	Chemical shift (δ) of H ₂ [ppm]	$d_{\text{H-H}}$ [Å] ^[35a] (from T ₁)
Cl ⁻ [2a]	dppe	-12.3	0.98
SC(SR)H	dppe	-8.55 to -8.71	0.94
PF(OR) ₂ ^{[a][3e]}	dppe	-5.12 to -5.63	0.94 to 0.97
PF ₃ ^[3a]	dppe	-4.33	0.92
H ⁻ [33]	dppe	-4.6	0.88
CO ^[1c]	dppp	-2.5	0.85

[a] R = Me, Et, O*i*Pr.

to be low. To confirm this phenomenon, the proton affinities of the dithioformate anion and that of the Ru complex were calculated at the B3LYP level. The proton affinity of the dithioformate anion was found to be approximately 340 kcal mol⁻¹. Interestingly, the proton affinity that corresponded to the dithioformate moiety coordinated to the Ru complex was found to have decreased to 251 kcal mol⁻¹.

The bonding between the ligand and the metal ion and their electronic manifestations on the dihydrogen moiety were analyzed by using the second-order perturbative interaction energies between natural bond orbitals obtained with the NBO analysis. The CO ligand was found to be the strongest π -acceptor (Ru→CO) among the ligands considered here with an interaction energy of about 23.6 kcal mol⁻¹, whereas the chlorido ligand acts as a π -donor (Cl→Ru) with an interaction energy of about 5.4 kcal mol⁻¹. Interestingly, the sulfur-based ligand, SC(SCH₃)H, was found to act both as a π -acceptor and as a π -donor. The corresponding interaction energies were calculated to be 1.5 (Ru→S=C) and 7.9 kcal mol⁻¹ (Ru←S), respectively. The effect of the change in these ligands on the bonding of the dihydrogen moiety to Ru was examined by analyzing the π back-donation from Ru to the σ^* orbital of H₂ (Table 4). The second-order perturbation interaction energies between the corresponding orbitals decreased as we moved from π -donor to π -acceptor and σ -donor ligands. In case of π -donor ligands, the back-donation from Ru to η^2 -H₂ is high, thereby resulting in large interaction energies. This trend illustrates the decrease in π back-donation along the series, thus further confirming the electronic effect discussed above. Notably, the interaction energy values for the SC(SCH₃)H ligand lies between those of π -donor and π -acceptor ligands, which shows dual character. Wiberg bond indices^[41] and overlap-weighted natural atomic orbital (NAO) bond orders^[42] were calculated, and those of select bonds are presented in Table 5. With respect to the change in the ligand *trans* to H₂, there seems to be no significant change in the bond orders/indices that correspond to the four Ru–P coordinations (Ru–P1, Ru–P2, Ru–P3, and Ru–P4 in Table 5). However, the bond orders between Ru and H₂, and between the two hydrogen atoms of the dihydrogen ligand (Ru–H₂ and H1–H2, respectively) change considerably with respect to the ligand. Similar to the trend in the

Table 5. Wiberg bond indices and overlap-weighted NAO bond orders for the Ru and the atoms to which it is bonded along with the bond orders for (η^2 -H₂) H–H atoms.

<i>trans</i> Ligand	Wiberg bond index					
	Ru–P1	Ru–P2	Ru–P3	Ru–P4	Ru–H ₂	H1–H2
Cl ⁻	0.771	0.772	0.772	0.771	0.670	0.549
SC(SCH ₃)H	0.781	0.767	0.766	0.782	0.621	0.573
H ⁻	0.785	0.790	0.790	0.785	0.49	0.682
CO	0.769	0.771	0.771	0.769	0.517	0.647
	NAO bond order					
Cl ⁻	0.766	0.763	0.763	0.766	0.872	0.546
SC(SCH ₃)H	0.765	0.744	0.745	0.762	0.843	0.565
H ⁻	0.793	0.795	0.796	0.793	0.735	0.623
CO	0.737	0.738	0.738	0.737	0.767	0.608

extent of back-donation, there is a correlation between the nature of the ligand and the calculated bond orders. Although NBO analysis gives an interpretation about the bonding in terms of orbital interactions, the topological analysis of electron density calculated using Bader's AIM approach^[43] results in a rigorous definition of chemical bonding using molecular graphs. In these graphs, the atoms that are bonded are linked by bond paths, and the minimum electron density along a bond path is termed as the bond critical point.^[44] AIM analysis was performed, and the bond critical points were located in a way that corresponded to all the bonds. In all the complexes, the Ru center is bonded to the η^2 -H₂ ligand through two bond critical points (BCPs), and these are intersected by two ring critical points (RCPs). In addition to this, there is also a bond critical point observed between the two hydrogen atoms in the η^2 -H₂ ligand. The electron density at the BCP (ρ), the Laplacian of the electron density ($\nabla^2\rho$), and the bond ellipticity (ϵ) values were obtained and compared with the experimental NMR spectroscopic chemical shifts given in Table 3. The correlation between several parameters calculated by using computational methods, and the chemical-shift values are presented in Figure 4. Linear correlations were obtained

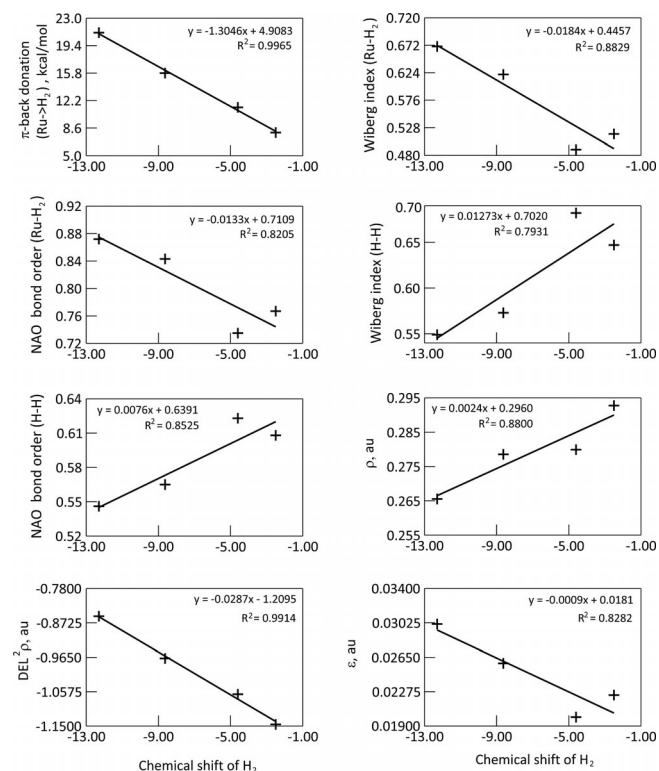


Figure 4. (a) Correlations of the interaction energies corresponding to the π back-donation from Ru to H₂ calculated by using the second-order perturbation analysis with NBO. (b) Wiberg index corresponding to the Ru–H₂ bond. (c) NAO bond order corresponding to the Ru–H₂ bond. (d) Wiberg index corresponding to the H–H bond. (e) NAO bond order corresponding to the H–H bond. (f) Electron density at the bond critical point corresponding to H–H. (g) Laplacian of the electron density at the bond critical point of H–H. (h) H–H bond ellipticity against the NMR spectroscopic chemical-shift values of the dihydrogen moiety.

for all the correlations with correlation coefficient values ranging from 0.83 to as good as 0.99. The *trans*-directing capability of the ligands under study [Cl⁻, SC(SCH₃)H, H⁻, CO] depends on the polarizability. Softer ligands have a remarkable *trans*-directing capability due to their high polarizability. The softer ligands like CO, H⁻, and RSH have good *trans*-directing ability when bound to the soft acid Ru⁺², because soft–soft interactions are favorable according to the hard/soft acid/base (HSAB) theory. The hard ligand Cl⁻, which has a low polarizability, has the least *trans*-directing ability. Bonding of the alkyl dithioformate ligand could be compared with the bonding of thiourea and thio-ketone to the metal atom. Fairlie et al.^[29] showed that thiourea in [(NH₃)₅Ru{SC(NH₂)₂}(S₂O₆)_{3/2}·H₂O] is a good π-donor ligand. Setkina and co-workers^[28] reported that the thiobenzylcyclopentadienyl ligand in [(η⁵-C₅H₅)-(CO)₂Mn←S=C(Ph)(C₅H₄)Mn(CO)₃] complexes shows both acceptor and donor properties. Hence the alkyl dithioformate/dithioformic acid bound to the metal atom is presumed to be a good π-acceptor and π-donor ligand. Our future plan is to study the lability and its mechanistic aspects, and the acidity of these dihydrogen ligands *trans* to sulfur-donor ligands.

Conclusion

The protonation reactions of the hydrido complexes *trans*-[Ru(H){SC(SR)H}(dppe)₂][X] (R = CH₃, X = OTf; R = C₆H₅CH₂, X = BPh₄; R = CH₂=CHCH₂, X = BPh₄; R = H, X = BF₄) with HBF₄·Et₂O result in new dicationic dihydrogen complexes, *trans*-[Ru(η²-H₂){SC(SR)H}(dppe)₂][X][BF₄]. H–H distances of all these dihydrogen complexes are of the order of 0.94 Å, thereby suggesting that there is no significant effect on the *d*_{H–H} value with a change in the electronics of the sulfur ligand. The reactivity of these dihydrogen complexes toward ligands such as CH₃CN and CO showed that the sulfur ligands are more labile than the bound H₂. The combined experimental and computational studies suggest that the sulfur ligands present in these *trans*-[Ru(η²-H₂){SC(SR)H}(dppe)₂][X][BF₄] dihydrogen complexes exhibit a poor π effect. The weak metal donor–acceptor interactions in the Ru–S bond could be further corroborated by the facile replacement of the sulfur ligand by H₂. The results from the density functional theory calculations and from the detailed analysis provide an excellent correlation between the NMR spectroscopic

chemical shifts that correspond to the dihydrogen moiety and the calculated parameter, which furthers our understanding of the bonding in this class of compounds.

Experimental Section

General Procedures: All reactions except those that involve the dihydrogen complexes were carried out under dry and purified nitrogen at room temperature by using standard Schlenk^[45] and inert-gas techniques unless otherwise specified. Manipulations that involved dihydrogen complexes were carried out under argon. Solvents used for the preparation of dihydrogen complexes were thoroughly saturated with argon just before use. ¹H and ³¹P{¹H} NMR spectroscopic data were acquired with a Bruker Avance 400 MHz spectrometer. The shifts of the residual protons of the deuterated solvents were used as internal reference. Variable-temperature ¹H spin–lattice relaxation time measurements were carried out at 400 MHz by using the inversion recovery method (180°-τ-90° pulse sequence at each temperature). The *T*₁ data are summarized in Table 1. ³¹P{¹H} NMR spectroscopic chemical shifts have been measured relative to 85% H₃PO₄ (aqueous solution) as an external standard in CD₂Cl₂. *trans*-[Ru(H){η¹-SC(S)H}(dppe)₂]^[46] and *trans*-[Ru(H){SC(SR)H}(dppe)₂][X]^[23] (R = CH₃, X = OTf; R = H₂C=CHCH₂, X = BPh₄; R = C₆H₅CH₂, X = BPh₄) were prepared according to literature methods.

The numbering scheme for the compounds reported in this work is summarized in Table 6.

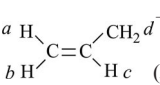
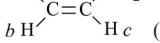
Table 6. Numbering scheme for the compounds.

L	H–H [Ru][X][BF ₄] SC(H)S(L)	H–D [Ru][X][BF ₄] SC(H)S(L)
CH ₃	1 ^[a]	[D]1 ^[a]
C ₆ H ₅ CH ₂	2 ^[b]	[D]2 ^[b]
H ₂ C=CHCH ₂	3 ^[b]	[D]3 ^[b]
H	4 ^[c]	[D]4 ^[c]

[a] X = OTf. [b] X = BPh₄. [c] X = BF₄; [Ru] = Ru(dppe)₂ fragment.

Preparation of *trans*-[Ru(η²-H₂){SC(SR)H}(dppe)₂][X][BF₄] [R = CH₃, X = OTf (1); R = C₆H₅CH₂, X = BPh₄ (2); R = CH₂=CHCH₂, X = BPh₄ (3); R = H, X = BF₄ (4)]: A 5 mm NMR spectroscopy tube charged with *trans*-[Ru(H){SC(SR)H}(dppe)₂][X] (0.02 g) was evacuated and filled with Ar in three cycles. The hydrido complex was then dissolved in CD₂Cl₂ (0.6 mL), and 54% HBF₄·Et₂O (5 equiv.) was added to this solution. The ¹H and ³¹P{¹H} NMR spectra revealed the formation of the dihydrogen

Table 7. ¹H and ³¹P{¹H} NMR spectroscopic data (δ) [ppm] of *trans*-[Ru(η²-H₂){SC(SR)H}(dppe)₂][X][BF₄] complexes in CD₂Cl₂.

R (compound)	Ru(η ² -H ₂)	R [SC(SR)H]	CH ₂ CH ₂ (dppe)	Ph (dppe)	P (dppe)
CH ₃ (1)	-8.68 (br. s, 2 H)	2.76 (s, 3 H, CH ₃), 7.83 [s, 1 H, SC(SCH ₃)H]	2.59 (m, 4 H), 3.17 (m, 4 H)	6.63–7.44 (m, 40 H)	52.4 (s)
C ₆ H ₅ CH ₂ (2)	-8.68 (br. s, 2 H)	4.43 [s, 2 H, SC(SH ₂ CC ₆ H ₅)H], 6.65–7.64 [m, 5 H, SC(SH ₂ CC ₆ H ₅)H], 7.83 [s, 1 H, SC(SH ₂ CC ₆ H ₅)H]	2.59 (m, 4 H), 3.17 (m, 4 H)	6.65–7.64 (m, 40 H)	52.4 (s)
^a H  ^d CH ₂ ^b H  ^c H (3)	-8.71 (br. s, 2 H)	3.85 [d, <i>J</i> (H ^a ,H ^c) = 6.8 Hz, 2 H, H ^a], 5.70 [d, <i>J</i> (H ^b ,H ^c) = 4.9 Hz, 1 H, H ^b], 5.73 [d, <i>J</i> (H ^a ,H ^c) = 5.9 Hz, 1 H, H ^a], 5.92 (m, 1 H, H ^c), 7.83 [s, 1 H, SC(SH ₂ CCH=CH ₂)H]	2.60 (m, 4 H), 3.16 (m, 4 H)	6.65–7.64 (m, 40 H)	52.3 (s)
H (4)	-8.55 (br. s, 2 H)	6.01 [d, <i>J</i> _{H,H} = 12.7 Hz, 1 H, SC(SH)H], 7.80 [d, <i>J</i> _{H,H} = 12.7 Hz, 1 H, SC(SH)H]	2.58 (m, 4 H), 3.19 (m, 4 H)	6.82–7.42 (m, 40 H)	52.5 (s)

complexes $trans\text{-}[\text{Ru}(\eta^2\text{-H}_2)\{\text{SC}(\text{SR})\text{H}\}(\text{dppe})_2][\text{X}][\text{BF}_4]$ [R = CH₃, X = OTf (1); R = C₆H₅CH₂, X = BPh₄ (2); R = CH₂=CHCH₂, X = BPh₄ (3); R = H, X = BF₄ (4)]. The NMR spectroscopic data of these derivatives are summarized in Table 7.

Observation of HD Isotopomers $trans\text{-}[\text{Ru}(\eta^2\text{-HD})\{\text{SC}(\text{SR})\text{H}\}(\text{dppe})_2][\text{X}][\text{BF}_4]$ (R = CH₃, X = OTf (D1); R = C₆H₅CH₂, X = BPh₄ (D2); R = CH₂=CHCH₂, X = BPh₄ (D3); R = H, X = BF₄ (D4)): These derivatives were prepared in the following manner: Each of the hydrido complexes 1, 2, 3, 4 (0.02 g) was dissolved in CD₂Cl₂ (0.6 mL) in a 5 mm NMR spectroscopy tube under Ar. Then 5 equiv. of 54% HBF₄·Et₂O was added. The ¹H NMR spectra revealed the complete conversion of the hydrido into the corresponding dihydrogen complexes D1, D2, D3, and D4. HD gas (generated from NaH and D₂O) was bubbled into the same solution for 5 min. The H–D isotopomer formed was observed by ¹H NMR spectroscopy.

Reaction of $trans\text{-}[\text{Ru}(\eta^2\text{-H}_2)\{\text{SC}(\text{SCH}_3)\text{H}\}(\text{dppe})_2][\text{OTf}][\text{BF}_4]$ (1) with CH₃CN: CH₃CN (2 equiv., 2 μL, 0.034 mmol) was added to a solution of 1 (0.02 g, 0.017 mmol) in CDCl₃. The yellow solution became pale. The ¹H and ³¹P NMR spectra revealed the complete conversion of 1 into $trans\text{-}[\text{Ru}(\eta^2\text{-H}_2)(\text{CH}_3\text{CN})(\text{dppe})_2][\text{OTf}][\text{BF}_4]$ accompanied by the elimination of SC(SCH₃)H. The yield of $trans\text{-}[\text{Ru}(\eta^2\text{-H}_2)(\text{CH}_3\text{CN})(\text{dppe})_2][\text{OTf}][\text{BF}_4]$ was 80% as ascertained from the ¹H NMR spectrum. ¹H NMR (CDCl₃) spectroscopic data of $trans\text{-}[\text{Ru}(\eta^2\text{-H}_2)(\text{CH}_3\text{CN})(\text{dppe})_2][\text{OTf}][\text{BF}_4]$: ¹H δ = –10.76 [br. s, 2 H, Ru–(η²-H₂)], 1.57 (s, 3 H, CH₃CN), 2.43 (br. m, 4 H, Ph₂PCH₂CH₂PPh₂), 3.01 (br. m, 4 H, Ph₂PCH₂CH₂PPh₂), 6.49–7.99 (m, 40 H, Ph₂PCH₂CH₂PPh₂) ppm. ³¹P{¹H} NMR (CDCl₃): δ = 56.6 (s, Ph₂PCH₂CH₂PPh₂) ppm.

Reaction of $trans\text{-}[\text{Ru}(\eta^2\text{-H}_2)\{\text{SC}(\text{SCH}_3)\text{H}\}(\text{dppe})_2][\text{OTf}][\text{BF}_4]$ (1) with CO: CO gas was purged for 2 min through a solution of 1 (0.02 g, 0.017 mmol) in CDCl₃. The yellow solution became paler. The ¹H and ³¹P NMR spectra revealed the complete conversion of 1 into $trans\text{-}[\text{Ru}(\text{H})(\text{CO})(\text{dppe})_2]^+$ accompanied by the elimination of SC(SCH₃)H.^[30] NMR spectroscopy evidenced the complete disappearance of the dihydrogen complex and the formation of $trans\text{-}[\text{Ru}(\text{H})(\text{CO})(\text{dppe})_2]^+$. ¹H NMR (CDCl₃) spectroscopic data for $trans\text{-}[\text{Ru}(\text{H})(\text{CO})(\text{dppe})_2]^+$: δ = –7.25 ppm (quint, 1 H, J_{H,P} = 19.6 Hz, Ru–H), 2.16 (br. m, 4 H, Ph₂PCH₂CH₂PPh₂), 2.47 (br. m, 4 H, Ph₂PCH₂CH₂PPh₂), 6.95–7.41 (m, 40 H, Ph₂PCH₂CH₂PPh₂). ¹³C{¹H} NMR (CDCl₃): δ = 32.2 (quint, J_{C,P} = 13.0 Hz, Ph₂PCH₂CH₂PPh₂), 128.4–133.7 (m, Ph₂PCH₂CH₂PPh₂), 200.5 (s, Ru–CO) ppm. ³¹P{¹H} NMR (CDCl₃): δ = 63.9 (s, Ph₂PCH₂CH₂PPh₂) ppm.

Reaction of $trans\text{-}[\text{Ru}(\eta^2\text{-H}_2)\{\text{SC}(\text{SCH}_3)\text{H}\}(\text{dppe})_2][\text{OTf}][\text{BF}_4]$ (1) with P(OCH₃)₃: P(OCH₃)₃ (3 equiv., 6 μL, 0.052 mmol) was added to a solution of 1 (0.02 g, 0.017 mmol) in CDCl₃. The color of the solution changed from yellow to orange. The ¹H and the ³¹P NMR spectra indicated the deprotonation of 1 to $trans\text{-}[\text{Ru}(\text{H})\{\text{SC}(\text{SCH}_3)\text{H}\}(\text{dppe})_2][\text{OTf}][\text{BF}_4]$. Then further P(OCH₃)₃ (2 equiv., 4 μL, 0.033 mmol) was added to this solution; the ¹H and the ³¹P NMR spectra revealed the formation of $trans\text{-}[\text{Ru}(\text{H})\{\text{PF}(\text{OCH}_3)_2\}(\text{dppe})_2][\text{OTf}][\text{BF}_4]$, SC(SCH₃)H and a small amount of $trans\text{-}[\text{Ru}(\text{H})\{\text{P}(\text{OCH}_3)_3\}(\text{dppe})_2][\text{OTf}][\text{BF}_4]$. The compounds SC(SCH₃)H, $trans\text{-}[\text{Ru}(\text{H})\{\text{PF}(\text{OCH}_3)_2\}(\text{dppe})_2][\text{OTf}][\text{BF}_4]$, and $trans\text{-}[\text{Ru}(\text{H})\{\text{P}(\text{OCH}_3)_3\}(\text{dppe})_2][\text{OTf}][\text{BF}_4]$ are present in a relative ratio of 1.00:0.77:0.23. ¹H NMR (CDCl₃) spectroscopic data for $trans\text{-}[\text{Ru}(\text{H})\{\text{PF}(\text{OCH}_3)_2\}(\text{dppe})_2][\text{OTf}][\text{BF}_4]$:^[3d] δ = –8.22 (dsept, 1 H, J_{H,P_{trans}} = 136.0, J_{H,P_{cis}} = 20.0, J_{H,F} = 20.0 Hz, Ru–H), 2.33 (m, 4 H, Ph₂PCH₂CH₂PPh₂), 2.71 (m, 4 H, Ph₂PCH₂CH₂PPh₂), 2.87 [d, 6 H, PF(OCH₃)₂], 6.58–7.81 (m, 40 H, Ph₂PCH₂CH₂PPh₂) ppm. ³¹P{¹H} NMR (CDCl₃): δ = 63.1 [d,

Ph₂PCH₂CH₂PPh₂, J_{P,P} = 32.0 Hz], 134.6 [dq, J_{P,F} = 1148.5, J_{P,P} = 32.0 Hz, PF(OCH₃)₂] ppm.

Computational Methods: Full geometry optimizations were carried out on a series of dihydrogen complexes bearing ligands [Cl[–], SC(SCH₃)H, H[–] and CO were chosen as model systems] that are present *trans* to η²-H₂ by using the density functional B3LYP^[47]/Genecp level (6-31G* basis set for C, H, O, P, S, Cl atoms and LANL2DZ^[48] basis set for Ru atoms) with the Gaussian 09 program.^[49] The data for the complexes at the B3LYP level using the Los Alamos effective core potential LANL2DZ basis set on all the atoms of the complexes considered are given in the Supporting Information. In all the calculations, the phenyl groups attached to the phosphorus atoms in the bidentate ligand were replaced by hydrogen atoms and were used as model systems. NBO analysis was performed to examine the bond orders, and the second-order perturbative energies for the donor–acceptor interactions. The NBO program 3.1^[41] included in the Gaussian 09 suite of programs was used for the analysis. The topological analysis of the electron density of these complexes was carried out by using the AIM method implemented in the AIMALL program.^[43] The anions surrounding the complex ions were not taken into account during optimization of these complexes at the B3LYP level.

Supporting Information (see footnote on the first page of this article): Experimental estimates of the H–H bond length and the interaction energy corresponding to π back-donation (Table S1); Wiberg bond indices and overlap-weighted NAO bond orders (Table S2); correlations of the interaction energies, Wiberg indices, NAO bond order, electron density, Laplacian values, and bond ellipticity (Figure S1); and Cartesian coordinates.

Acknowledgments

We thank the Department of Science and Technology, New Delhi (India) (no. SR/FT/CS-135/2011) for financial support. T. G. is very grateful to Prof. Balaji R. Jagirdar, IISc, Bangalore, India, for intellectual discussions. V. P. thanks the Department of Science and Technology (DST) for an INSPIRE fellowship.

- a) K. D. Welch, W. G. Dougherty, W. S. Kassel, D. L. DuBois, R. M. Bullock, *Organometallics* **2010**, *29*, 4532; b) S. Bolano, J. Bravo, F. Fernandez-Garcia, S. Garcia-Fontan, C. M. M. Del, *J. Organomet. Chem.* **2009**, *694*, 2994; c) E. Rocchini, A. Mezzetti, H. Ruegger, U. Burckhardt, V. Gramlich, Z. A. Del, P. Martinuzzi, P. Rigo, *Inorg. Chem.* **1997**, *36*, 711.
- a) S. Dutta, B. R. Jagirdar, *J. Chem. Sci. (Bangalore, India)* **2006**, *118*, 579; b) B. Chin, A. J. Lough, R. H. Morris, C. T. Schweitzer, C. D'Agostino, *Inorg. Chem.* **1994**, *33*, 6278.
- a) H. V. Nanishankar, M. Nethaji, B. R. Jagirdar, *Eur. J. Inorg. Chem.* **2004**, 3048; b) G. Albertin, S. Antoniutti, A. Bacchi, C. D'Este, G. Pelizzi, *Inorg. Chem.* **2004**, *43*, 1336; c) C. M. Nagaraja, M. Nethaji, B. R. Jagirdar, *Inorg. Chem. Commun.* **2004**, *7*, 654; d) N. Mathew, B. R. Jagirdar, A. Ranganathan, *Inorg. Chem.* **2003**, *42*, 187; e) N. Mathew, B. R. Jagirdar, R. S. Gopalan, G. U. Kulkarni, *Organometallics* **2000**, *19*, 4506; f) N. Mathew, B. R. Jagirdar, *Inorg. Chem.* **2000**, *39*, 5404.
- T. P. Fong, C. E. Forde, A. J. Lough, R. H. Morris, P. Rigo, E. Rocchini, T. Stephan, *J. Chem. Soc., Dalton Trans.* **1999**, 4475.
- a) V. Sivakumar, M. Nethaji, B. R. Jagirdar, N. Mathew, *Synth. React. Inorg. Met.-Org. Nano-Met. Chem.* **2007**, *37*, 677; b) K. K. Majumdar, H. V. Nanishankar, B. R. Jagirdar, *Eur. J. Inorg. Chem.* **2001**, 1847.
- M. A. Esteruelas, L. A. Oro, N. Ruiz, *Inorg. Chem.* **1993**, *32*, 3793.
- M. J. Albeniz, M. L. Buil, M. A. Esteruelas, A. M. Lopez, L. A. Oro, B. Zeier, *Organometallics* **1994**, *13*, 3746.

- [8] D. Sellmann, T. Gottschalk-Gaudig, F. W. Heinemann, *Inorg. Chem.* **1998**, *37*, 3982.
- [9] D. Sellmann, A. Hille, A. Roesler, F. W. Heinemann, M. Moll, G. Brehm, S. Schneider, M. Reiher, B. A. Hess, W. Bauer, *Chem. Eur. J.* **2004**, *10*, 819.
- [10] a) M. Schlaf, A. J. Lough, R. H. Morris, *Organometallics* **1996**, *15*, 4423; b) M. Schlaf, R. H. Morris, *J. Chem. Soc., Chem. Commun.* **1995**, 625; c) M. Schlaf, A. J. Lough, R. H. Morris, *Organometallics* **1993**, *12*, 3808.
- [11] H. Li, X. Wang, F. Huang, G. Lu, J. Jiang, Z.-X. Wang, *Organometallics* **2011**, *30*, 5233.
- [12] a) C. F. Lovitt, G. Frenking, G. S. Girolami, *Organometallics* **2012**, *31*, 4122; b) N. V. Belkova, L. M. Epstein, E. S. Shubina, *Eur. J. Inorg. Chem.* **2010**, 3555; c) D. S. Nemcsok, A. Kovács, V. M. Rayón, G. Frenking, *Organometallics* **2002**, *21*, 5803.
- [13] a) R. H. Morris, *Coord. Chem. Rev.* **2008**, *252*, 2381; b) G. B. Bacsikay, I. Bytheway, N. S. Hush, *J. Am. Chem. Soc.* **1996**, *118*, 3753.
- [14] a) G. Kovács, A. Rossin, L. Gonsalvi, A. Lledós, M. Peruzzini, *Organometallics* **2010**, *29*, 5121; b) C. M. Nagaraja, P. Parameswaran, E. D. Jemmis, B. R. Jagirdar, *J. Am. Chem. Soc.* **2007**, *129*, 5587.
- [15] F. Maseras, A. Lledós, E. Clot, O. Eisenstein, *Chem. Rev.* **2000**, *100*, 601.
- [16] Z. Xu, I. Bytheway, G. Jia, Z. Lin, *Organometallics* **1999**, *18*, 1761.
- [17] D. Burgos, C. Olea-Azar, F. Mendizabal, *J. Mol. Model.* **2012**, *18*, 2021.
- [18] J. Li, P. Pykko, *Inorg. Chem.* **1993**, *32*, 2630.
- [19] S. Canales, O. Crespo, M. C. Gimeno, P. Jones, A. Laguna, F. Mendizabal, *Organometallics* **2001**, *20*, 4812.
- [20] O. Haberlen, S. C. Shung, N. Rösch, *Int. J. Quantum Chem. Quantum Chem. Symp.* **1994**, *28*, 595.
- [21] O. Haberlen, N. Rösch, *J. Phys. Chem.* **1993**, *97*, 4970.
- [22] T. Y. Bartucz, A. Golombek, A. J. Lough, P. A. Maltby, R. H. Morris, R. Ramachandran, M. Schlaf, *Inorg. Chem.* **1998**, *37*, 1555.
- [23] a) T. Gandhi, M. Nethaji, B. R. Jagirdar, *Inorg. Chem.* **2003**, *42*, 4798; b) T. Gandhi, B. R. Jagirdar, *Inorg. Chem.* **2005**, *44*, 1118.
- [24] a) A. G. Vandeputte, M. K. Sabbe, M.-F. Reyniers, G. B. Marin, *Chem. Eur. J.* **2011**, *17*, 7656; b) M. T. Nguyen, T. L. Nguyen, H. T. Le, *J. Phys. Chem. A* **1999**, *103*, 5758; c) J.-H. Huang, K.-L. Han, R.-S. Zhu, G.-Z. He, N.-Q. Lou, *J. Phys. Chem. A* **1998**, *102*, 2044; d) Y. G. Smeyers, M. Villa, G. I. Cardenas-Jiron, A. Toro-Labbe, *THEOCHEM* **1998**, *426*, 155; e) E. D. Jemmis, K. T. Giju, J. Leszczynski, *J. Phys. Chem. A* **1997**, *101*, 7389; f) M. Remko, K. R. Liedl, B. M. Rode, *Chem. Phys. Lett.* **1996**, *263*, 379; g) X. Xie, Y. Tao, H. Cao, W. Duang, *Chem. Phys.* **1996**, *213*, 133.
- [25] a) B. Bak, O. Nielsen, H. Svanholt, J. J. Christiansen, *J. Mol. Spectrosc.* **1979**, *75*, 134; b) B. Bak, O. J. Nielsen, H. Svanholt, *J. Mol. Spectrosc.* **1978**, *69*, 401.
- [26] F. Ioannoni, D. C. Moule, J. D. Goddard, D. J. Clouthier, *J. Mol. Struct.* **1989**, *197*, 159.
- [27] P. Barrio, M. A. Esteruelas, E. Onate, *Organometallics* **2002**, *21*, 2491.
- [28] V. G. Andrianov, Y. T. Struchkov, P. V. Petrovskii, E. I. Fedin, D. N. Kursanov, S. P. Dolgova, V. N. Setkina, *J. Organomet. Chem.* **1981**, *221*, 183.
- [29] D. P. Fairlie, W. A. Wickramasinghe, K. A. Byriel, H. Taube, *Inorg. Chem.* **1997**, *36*, 2242.
- [30] A. Santos, J. Lopez, J. Montoya, P. Noheda, A. Romero, A. M. Echavarren, *Organometallics* **1994**, *13*, 3605.
- [31] G. J. Kubas, *Adv. Inorg. Chem.* **2004**, *56*, 127.
- [32] H. Binder, R. Fischer, *Z. Naturforsch. B* **1972**, *27*, 753.
- [33] a) M. T. Bautista, E. P. Cappellani, S. D. Drouin, R. H. Morris, C. T. Schweitzer, A. Sella, J. Zubkowski, *J. Am. Chem. Soc.* **1991**, *113*, 4876; b) M. T. Bautista, K. A. Earl, P. A. Maltby, R. H. Morris, C. T. Schweitzer, A. Sella, *J. Am. Chem. Soc.* **1988**, *110*, 7031.
- [34] A. C. Albeniz, D. M. Heinekey, R. H. Crabtree, *Inorg. Chem.* **1991**, *30*, 3632.
- [35] a) P. A. Maltby, M. Schlaf, M. Steinbeck, A. J. Lough, R. H. Morris, W. T. Klooster, T. F. Koetzle, R. C. Srivastava, *J. Am. Chem. Soc.* **1996**, *118*, 5396; b) B. Chin, A. J. Lough, R. H. Morris, C. T. Schweitzer, C. D'Agostino, *Inorg. Chem.* **1994**, *33*, 6278.
- [36] M. S. Chinn, D. M. Heinekey, N. G. Payne, C. D. Sofield, *Organometallics* **1989**, *8*, 1824.
- [37] a) T. Hasegawa, Z. Li, S. Parkin, H. Hope, R. K. McMullan, T. F. Koetzle, H. Taube, *J. Am. Chem. Soc.* **1994**, *116*, 4352; b) B. Moreno, S. Sabo-Etienne, B. Chaudret, A. Rodriguez-Fernandez, F. Jalon, S. Trofimenko, *J. Am. Chem. Soc.* **1994**, *116*, 2635; c) J. P. Collman, P. S. Wagenknecht, J. E. Hutchison, N. S. Lewis, M. A. Lopez, R. Guillard, M. L'Her, A. A. Bothner-By, P. K. Mishra, *J. Am. Chem. Soc.* **1992**, *114*, 5654.
- [38] T. A. Luther, D. M. Heinekey, *Inorg. Chem.* **1998**, *37*, 127.
- [39] D. M. Heinekey, W. J. Oldham Jr., *J. Am. Chem. Soc.* **1994**, *116*, 3137.
- [40] G. J. Kubas, *J. Organomet. Chem.* **2001**, *635*, 37.
- [41] F. L. Weinhold, C. R. Landis, *Valency and Bonding. A Natural Bond Orbital Donor-Acceptor Perspective*, Cambridge University Press, Cambridge, **2005**.
- [42] K. B. Wiberg, *Tetrahedron* **1968**, *24*, 1083.
- [43] a) A. E. Reed, R. B. Weinstock, F. Weinhold, *J. Chem. Phys.* **1985**, *83*, 735; b) A. E. Reed, F. Weinhold, *J. Chem. Phys.* **1983**, *78*, 4066.
- [44] a) T. A. Keith, *AIMAll*, Version 11.12.19, aim.tkgristmill.com, **2011**; b) R. F. W. Bader, *Atoms in Molecules: A Quantum Theory*, Oxford University Press, Oxford, **1990**.
- [45] a) D. F. D. Shriver, M. A. Drezdzonek, *The Manipulation of Air Sensitive Compounds*, 2nd ed., Wiley, New York, **1986**; b) S. Herzog, J. Dehnert, K. Lühder, in *Technique of Inorganic Chemistry* (Ed.: H. B. Johnassen), Interscience, New York, **1969**, vol. VII.
- [46] T. Gandhi, M. Nethaji, B. R. Jagirdar, *Inorg. Chem.* **2003**, *42*, 667.
- [47] a) A. D. Becke, *Phys. Rev. A* **1988**, *38*, 3098; b) C. Y. W. Lee, R. G. Parr, *Phys. Rev. B* **1988**, *37*, 785.
- [48] T. H. Dunning, P. J. Hay, in *Modern Theoretical Chemistry* (Eds.: H. F. Schaefer III), Plenum, New York, **1976**, vol. 3, p. 1.
- [49] M. J. Frisch, G. W. Trucks, H. B. Schlegel, G. E. Scuseria, M. A. Robb, J. R. Cheeseman, G. Scalmani, V. Barone, B. Mennucci, G. A. Petersson, H. Nakatsuji, M. Caricato, X. Li, H. P. Hratchian, A. F. Izmaylov, J. Bloino, G. Zheng, J. L. Sonnenberg, M. Hada, M. Ehara, K. Toyota, R. Fukuda, J. Hasegawa, M. Ishida, T. Nakajima, Y. Honda, O. Kitao, H. Nakai, T. Vreven, J. A. Montgomery Jr., J. E. Peralta, R. Ogliaro, M. Bearpark, J. J. Heyd, E. Brothers, K. N. Kudin, V. N. Staroverov, R. Kobayashi, J. Normand, K. Raghavachari, A. Rendell, J. C. Burant, S. S. Iyengar, J. Tomasi, M. Cossi, N. Rega, J. M. Millam, M. Klene, J. E. Knox, J. B. Cross, V. Bakken, C. Adamo, J. Jaramillo, R. Gomperts, R. E. Stratmann, O. Yazyev, A. J. Austin, R. Cammi, C. Pomelli, J. W. Ochterski, R. L. Martin, K. Morokuma, V. G. Zakrzewski, G. A. Voth, P. Salvador, J. J. Dannenberg, S. Dapprich, A. D. Daniels, Ö. Farkas, J. B. Foresman, J. V. Ortiz, J. Cioslowski, D. J. Fox, *Gaussian 09*, Revision A.01, Gaussian, Inc., Wallingford, CT, **2009**.

Received: September 5, 2012

Published Online: February 1, 2013